Quantitative analysis of cell adhesion on aligned micro- and nanofibers

Furong Tian,[1,7] Hossein Hosseinkhani,[2] Mohsen Hosseinkhani,[3] Ali Khademhosseini,[4,5] Yoshiro Yokoyama,[1] Giovani Gomez Estrada,[6] Hisatoshi Kobayashi[1,8]

[1]*Biomaterials Center, National Institute for Materials Science (NIMS), Tsukuba, Ibaraki 305-0044, Japan*
[2]*International Center for Young Scientists (ICYS), National Institute for Materials Science (NIMS), Tsukuba, Ibaraki 305-0044, Japan*
[3]*Department of Cardiovascular medicine, Graduate School of Medicine, Kyoto University Hospital, Kyoto 606-8507, Japan*
[4]*Harvard-MIT Division of Health Sciences and Technology, Massachusetts Institute of Technology (MIT), Cambridge, Massachusetts 02139*
[5]*Center for Biomedical Engineering, Department of Medicine, Brigham and Women's Hospital, Harvard Medical School, Cambridge, Massachusetts 02139*
[6]*Max-Planck Institute for Metals Research, Heisenberg St. 3, Stuttgart 70569, Germany*
[7]*Institute for Inhalation Biology GSF-Research Center for Environment and Health, Ingolstaedter Landstrasse 1, D-85764 Neuherberg/Munich, Germany*
[8]*Institute of Biomaterials and Bioengineering, Tokyo Medical and Dental University, Tokyo 113-8549, Japan*

Received 29 August 2006; revised 4 December 2006; accepted 3 January 2007
Published online 2 July 2007 in Wiley InterScience (www.interscience.wiley.com). DOI: 10.1002/jbm.a.31304

Abstract: In this study, we quantitatively analyzed the affinity of cell adhesion to aligned nanofibers composed of composites of poly(glycolic acid) (PGA) and collagen. Electrospun composite fibers were fabricated at various PGA/collagen weight mixing ratio (7, 18, 40, 67, and 86%) to generate fibers that ranged in diameter from 10 μm to 500 nm. Scanning electron microscopy (SEM) observation revealed that the PGA/collagen fibers were long and uniformly aligned, irrespective of the PGA/collagen weight mixing ratio. In addition, it was observed that a significantly higher number of NIH3T3 fibroblasts adhered to nanofibers with smaller diameters in comparison to fibers with larger diameters. The highest affinity of cell adhesion was observed in the PGA/collagen fibers with diameter of 500 nm and PGA/collagen weight mixing ratio of 40%. Furthermore, the adherent cells were more elongated on fibers with smaller diameters. Thus, based on the results here, PGA/collagen composite fibers are suitable for tissue culture studies and provide an attractive material for tissue engineering applications. © 2007 Wiley Periodicals, Inc. J Biomed Mater Res 84A: 291–299, 2008

Key words: quantitative; fibroblast; fiber; poly(glycolic acid) (PGA); collagen

INTRODUCTION

The healing of full-thickness skin defects requires extensive synthesis and remodeling of dermal and epidermal components. Fibroblasts play an important role in this process and are being incorporated in the latest generation of artificial dermal substitutes. Materials design of scaffold for cell proliferation and differentiation is one of the key technologies for tissue engineering. To obtain the desired cell response from a biomaterial, the chemical, mechanical, and the structure of the material must be optimized. In most cases, these properties must be engineered to generate a suitable environment for controlling cell adhesion and attachment.[1] Many biodegradable synthetic polymers, such as PGA and its copolymers with L-lactic acid, D,L-lactic acid, and ε-caprolactone have been fabricated into scaffolds for tissue engineering applications.[2–4] Nanofibers may provide a suitable material for tissue engineering since they can be used to enhance cell adhesion. In particular, the diameters of fibers play an important

Correspondence to: H. Kobayashi; e-mail: kobayashi.hisatoshi@nims.go.jp
Contract grant sponsor: Research Promotion Bureau; contract grant numbers: 17-083, 18-457
Contract grant sponsor: Ministry of Education, Culture, Sports, Science and Technology (MEXT), Japan

role in the adhesion of the cells to the fibers. Takahashi and Tabata compared the attachment of mesenchymal stem cells on microscale nonwoven polyethylene terephthalate (PET) fibers prepared with different diameters.[5] Furthermore, it has been demonstrated that polyaniline (PANi) and poly (D,L-lactide-*co*-glycolide) (PLGA) fibers that ranged in diameter from 500 to 800 nm enhanced cell adhesion.[6–10] Also, poly(ε-caprolactone) nanofibers (diameter = 700 nm) were shown to be a suitable carrier for mesenchymal stem cells transplantation.[11] However, it is not yet clear how the diameter of the fibers affect tissue engineering scaffolds for skin regeneration.

Electrospinning is a common technique used to fabricate tissue engineering scaffolds. Recently, several studies have demonstrated the use of electrospinning for fabrication of aligned polymeric nanofibers.[12–14] It has been reported that this electrospun scaffolds can be used to generated aligned nanofibers (300 nm) of poly(L-lactic acid) (PLLA), which improve the differentiation of neural stem cells (NSC) and support neuronal outgrowth in comparison to fibers with larger diameters.[15] Therefore, the availability of aligned nanofibers can be potentially useful in tissue engineering.

The adhesion of NIH-3T3 fibroblasts has been studied on poly(*p*-dioxanone-*co*-L-lactide)-*block*-poly (ethylene glycol) (PPDO/PLLA-*b*-PEG) nanofibers.[16] However, there are no studies on the interaction of individual cells and nanofibers in a systematic manner. To study the mechanism of interaction between cells and nanofibers, it is important to control the architecture of nanofibers to minimize the interaction of a single cell with the neighboring fibers. Therefore, aligned micro- and nanofibers in which the adherent cells only interact with individual fibers is a potentially useful approach for studies that aim to analyze such interactions.[17] However, it is not yet clear about the factors that affect on cell adhesion between materials and extracellular matrix (ECM) proteins. To study the effect of fiber diameter on the adhesion of fibroblast cells, a quantitative electrospinning model was set up. In this study, we used a number of biomaterials that are commonly used in tissue engineering and are natural components of the cellular microenvironment. Specifically, we used PGA, a well-known biomaterial and collagen, which is one of the main components of the ECM.[1,10] Electrospun composite nanofibers comprising various ratios of PGA and collagen were fabricated with diameters in the range of 10 μm, 3–5 μm, and 500 nm. We analyzed the properties of NIH-3T3 cells on these fibers as a function of fiber diameter and structure. It was demonstrated that the fiber composition and diameter have a direct influence on the morphology and alignment of the fibroblast cells, indicating that fiber properties can be used for engineering scaffolds that induce specific functional properties on seeded cells.

MATERIALS AND METHODS

Materials

PGA was purchased from Polysciences, USA. Collagen was purchased from Nippon Meat Packers. 1,1,1,3,3,3-Hexafluroro-2-2-propanol was supplied by Merck KGaA, Germany. Phosphate buffer saline (PBS, pH 7.4), Dulbecco's modified Eagle medium (DMEM), mouse I_gG antivicullin, and sheep anti-mouse-Cy3 antibody were obtained from Sigma Chemical (St. Louis, MO).

Fabrication of fibrous scaffold

Solutions for electrospinning were prepared by mixing PGA and collagen solution. PGA solution was prepared by dissolving 67 mg of PGA in 100 mL of 1,1,1,3.3.3 hexafluroro-2-2-propanol under stirring at 80°C for 48 h. Collagen solution was prepared by dissolving 100 mg of collagen in 100 mL of 1,1,1,3,3,3 hexafluroro-2-2-propanol under stirred condition at 4°C for 12 h. Immediately before electrospinning, samples were prepared by mixing two solutions at volume mixing ratio of PGA to collagen at 1:9, 2.5:7.5, 5:5, 7.5:2.5, and 9:1, respectively. The calculated concentrations for each of the components in the various samples are listed in Table I. The mixture solution was delivered by a programmable pump (Harvard Apparatus, MA) to the exit hole of the electrode (Spinneret with a hole diameter of 0.7 mm). The flow rate was set to 10 mL/h. A high-voltage power supply (Nippon-stabilizer industry) was used to provide the necessary voltage for the fabrication of fibers. The voltages of power supply and distances from spinneret and collector, which were controlled for getting precise diameter of fibers, are listed in Table II. The diameter of drum was 15 cm in diameter with a 2 cm diameter hole cut in the center. A stepper motor (EYELA MAZELA Z., Tokyo, Rikakikai, Japan) was used to control the speed of the drum. The grounded platform for collecting the fibers was a PVA. The mandrel was rotated at 1200 rpm to generate aligned fibers. The PGA-collagen fibers was removed from the mandrel and processed for scan-

TABLE I
The Concentration of PGA and Collagen in Mixed Solution

PGA:Collagen Ratio (v/v)	Mass in 100 mL HFP (mg)		PGA Mixing Weight Ratio (w/w) (%)
	PGA	Collagen	
90:10	60.30	10	86
75:25	50.25	25	67
50:50	33.5	50	40
25:75	16.75	75	18
10:90	6.7	90	7

TABLE II
The Voltage of Power Supply and Distance Between Spinneret and Collector Control the Diameter of Fibers

	Diameter of Fiber		
	10 μm	3–5 μm	500 nm
Voltage of power supply (kV)	23	26	26
Distance from spinneret to collector (cm)	18	18	23

ning electron microscopy (SEM). The only processing required for the SEM analysis was sputter coating, since the fibrous structures produced were completely dry after electrospinning. Micrographs from the SEM analysis were digitized and analyzed by JEOL EDSEM., Tokyo, Japan.

Cell culture

NIH-3T3 fibroblasts were cultured at 37°C in a 95% air and 5% CO_2 atmosphere. Dulbeccos' modified Eagle's medium (DMEM) supplemented with 10% fetal bovine serum (FBS, GIBCO, BRL) was used as the cell culture medium and was changed every 2 days. To subculture, cells were trypsinized and subsequently seeded into each well of 12-well tissue culture plates (Code 3800-6100, Iwaki brand; Scitech Division of Asahi Techno Glass, Chiba, Japan) at a density of 2×10^4 cell/cm^2.

Cell seeding on the PGA/collagen fibers

PGA/collagen fibers were sterilized in ethylene oxide gas (EOG) for 22 h and then washed three times with PBS (pH 7.4) to remove residual 1,1,1,3,3,3 hexafluroro-2-2 propanol. NIH-3T3 cells at various concentrations (1×10^2 to 1×10^4 cell/mL) were seeded randomly on aligned macro- or nanofibers and cultured for 1 h in DMEM without serum and then gently washed with serum-free DMEM. The number of cells attached were counted and normalized to the length of the fibers.

Immunocytochemical analysis

The adhered cells on the fibers were incubated for 8 h in DMEM supplement with 10% FBS. Immunocytochemical analysis was used to evaluate the morphology of adhered cells.[18] Briefly, the samples were fixed with methanol for 20 min, and then washed with PBS, and permeabilized with 0.2% Triton X-100 for 5 min at room temperature. The samples were then incubated in 1% bovine serum albumin (BSA) dissolved in PBS for 1 h. Samples were incubated with the primary antibody, i.e. mouse I_gG antivicullin (1:2000 dilution, Sigma), then washed with PBS and then incubated with sheep anti-mouse-Cy3 antibody (1:200) for 30 min. The samples were mounted on *N*-propyl/gallate/glycerol and examined under fluorescent microscope (Zeiss, Germany). The number of cells and their length adhered on the fibers were quantified on 2 mm aligned fibers.

Confocal microscopy

Cells were visualized using a Zeiss inverted confocal microscope (LSM 510, Carl Zeiss). A typical stack of optical sections (z-series) through NIH-3T3 cells reveal internal variations in fluorescence emission wavelengths in the right and top of the image. Optical sections were gathered in increments of 0.01 μm steps perpendicular to the *z*-axis (microscope optical axis) using helium–neon (543 nanometer; red fluorescence) laser system.

Statistical analysis

Differences between experimental groups and the control groups were evaluated using the statistical analysis package SPSS 11. The $p < 0.05$ was accepted to be significant. A one-way Analysis of Variance (ANOVA) was used to test the difference between the groups. Exploratory data analyses were performed with Kolmogorov–Smirnov tests as to validate the normality assumption found in ANOVA and *t*-tests.

RESULTS

In this study, we analyzed the fabrication of aligned nanofibers composed of PGA/collagen composite materials. As shown in Figure 1(A), PGA/collagen nanofibers could be fabricated to generate randomly aligned structure of PGA/collagen fibers. Furthermore, the alignment of nanofibers could be aligned by using a spinning substrate [Fig. 1(B)].

Figure 2(A) shows a typical photomicrograph of aligned PGA/collagen fiber (40% ratio). As it can be seen, the fibers are aligned parallel to each other at a distance of ~200 μm. Also, as shown in Figure 2(B), cells adhered along the nanofibers after 1 h in DMEM medium. We also quantified the degree of cell adhesion onto the nanofibers by measuring the number of cells that adhered onto each fiber as a function of the initial cell seeding density (Fig. 3). There was a linear trend between the number of cells seeded and the number of cells that were adhered on the nanofiber scaffolds.

To determine the effect of fiber diameter on the cell adhesion, we fabricated fibers made from different diameters (10 μm, 3–5 μm, and 500 nm) and seeded NIH-3T3 cells on the resulting aligned nanofibers for 8 h in the DMEM medium supplemented with 10% FBS. As shown in Figure 4(A–C), cells aligned and adhered on fibers with various cell concentrations. These experiments were performed for fibers made from various compositions of PGA/collagen composite materials and various diameter

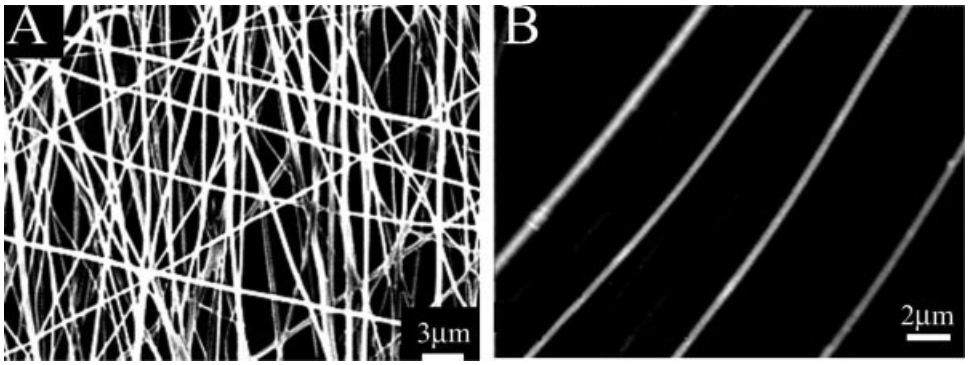

Figure 1. Scanning electron micrographs of the structural morphology of PGA/collagen fibers. A: PGA/collagen fiber fabricated by electrospinning process showing a random of fibers with a diameter of 500 nm. B: Aligned fibers collected on PVA collecting fibers with diameter of 500 nm.

fibers. Figure 5 shows the quantified results of the number of cells that adhered on the fibers for these conditions. There were no significant differences between the numbers of cells that adhered to fibers with diameter of 10 μm or 3–5 μm for the various composition polymers used in this study. However, there was a significant difference between the numbers of cells attached to fibers with diameter bigger than 3 μm and 500 nm ($p < 0.01$). This increased adhesion for smaller fibers was independent of the material used. It is important to note that the 40% composition of the PGA/collagen composite material had a higher level of cell adhesion and mechanical properties associated with the resulting scaffolds and was therefore used for subsequent studies.

We also examined the effects of nanofiber structure on the morphology of the adhered cells. NIH-3T3 cells obtained a more spherical and rounded morphology upon adhesion to the fibers with larger

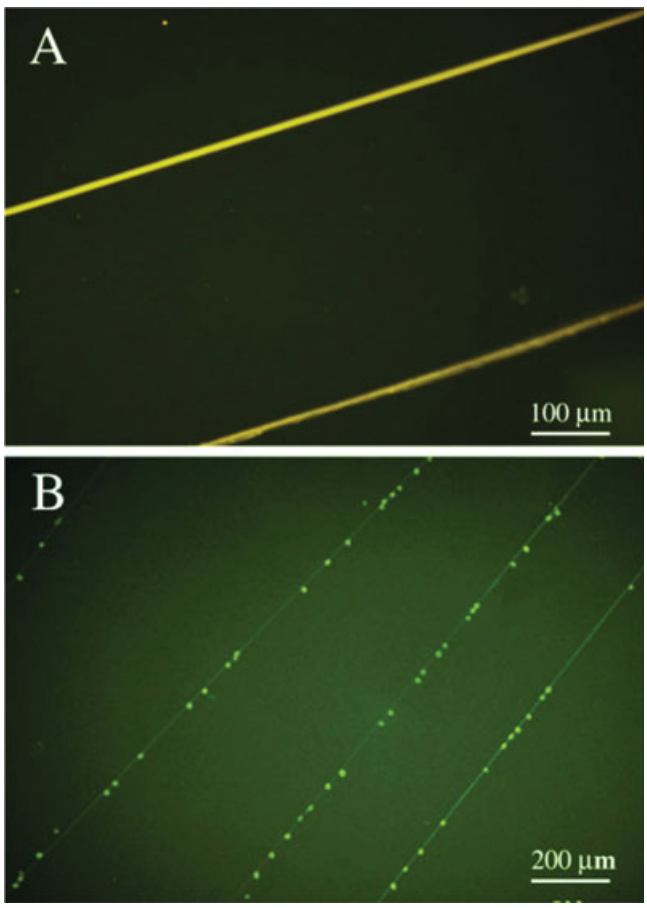

Figure 2. Morphology of PGA/collagen fibers and cells examined by fluorescent microscopy. A: Photography of PGA/collagen fibers. B: Images showing NIH-3T3 cells seeded on the PGA/collagen fibers. [Color figure can be viewed in the online issue, which is available at www.interscience.wiley.com.]

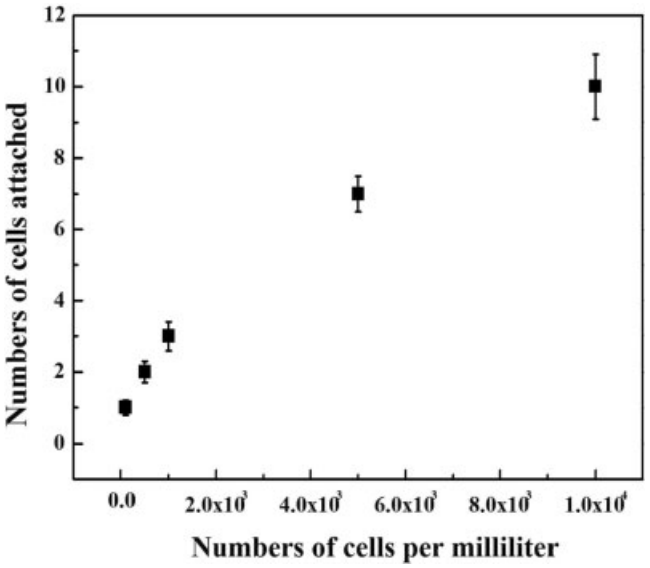

Figure 3. The relationship between cell seeding concentration and the number of attached cells on the fibers. The averages of the cells number presenting the numbers of cells attached on the fiber among different concentrations of cells in the medium (numbers/milliliter). The experiments were performed independently five times. Error bars show the standard deviation.

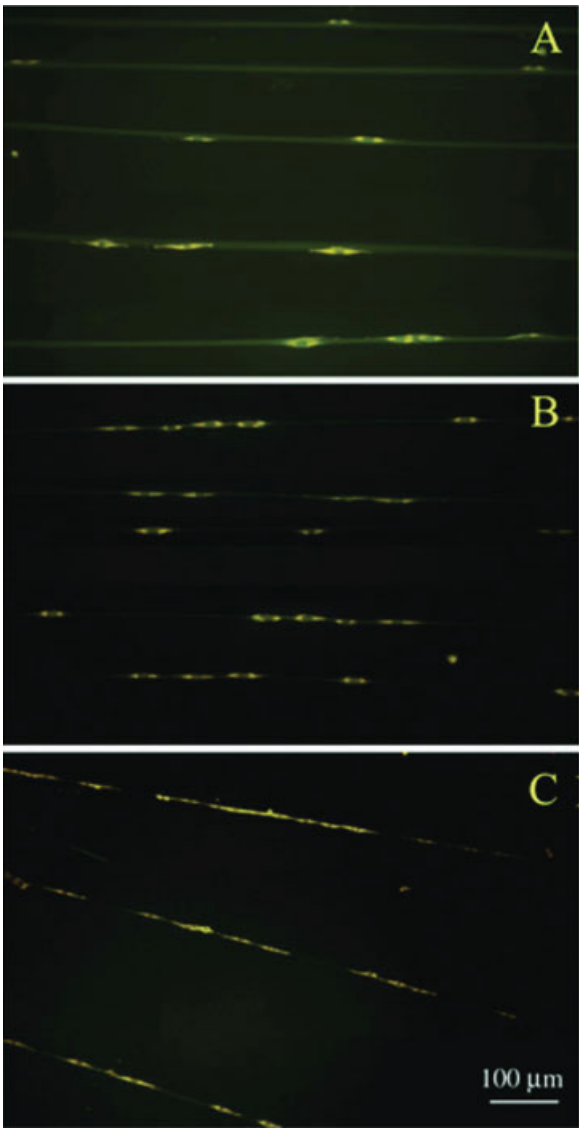

Figure 4. Morphology of cells and fibers examined by fluorescent microscopy. Photographs showing different amount of cells adhered on PGA/collagen fibers at weight mixing ratio of 40% with diameter of (A) 10 μm; (B) 3–5 μm; (C) 500 nm. [Color figure can be viewed in the online issue, which is available at www.interscience.wiley.com.]

diameters [Fig. 6(A)]. In comparison, the cells that adhered to smaller diameters were more spread out and elongated [Fig. 6(B,C)]. We quantified the spreading of the cells on nanofibers of various shapes and sizes to determine the relationship between cell length and the fiber diameter (Fig. 7). The quantified results confirmed the visual inspection analysis that there is a significant difference between the smaller diameter nanofibers (500 nm) compared with larger diameter fibers ($p < 0.01$).

We also examined the effects of nanofiber chemistry on the length of the adhered cells. In these studies, we analyzed the length of the adhered cells as a function of the PGA/collagen ratio. As shown in Figure 8, cells spread in a biphasic manner at various compositions of the PGA/collagen mixtures. In these studies, cells that were on composite materials that composed of 7 or 86% PGA contained cells that were less spread in comparison to composites that had a PGA concentration of 40%.

To further determine the alignment of the cells on the nanofibers, cells were imaged using confocal microscopy (Fig. 9). *X*–*Y* axis shows the cell adhered on the fiber with diameter of 500 nm in the middle of image. The top of confocal microscopy image (*Z*-axis) shows round shape, which presents vertical section of cylindrical cell body. *Z*-axis image shows that nanofiber is underneath the cell and cell internalized into the fiber.

DISCUSSION

PGA/collagen nanofibers provide a potentially useful material for tissue engineering due to their biocompatibility, degradability, and biologically relevant nature. However, despite much promise as a tool for tissue engineering, there is gap in understanding the nature of the cell adhesion on electrospun nanofibers. Here, we aimed to study the effects of fiber diameter and composition on the resulting cell adhesion and morphology. Specifically, to avoid

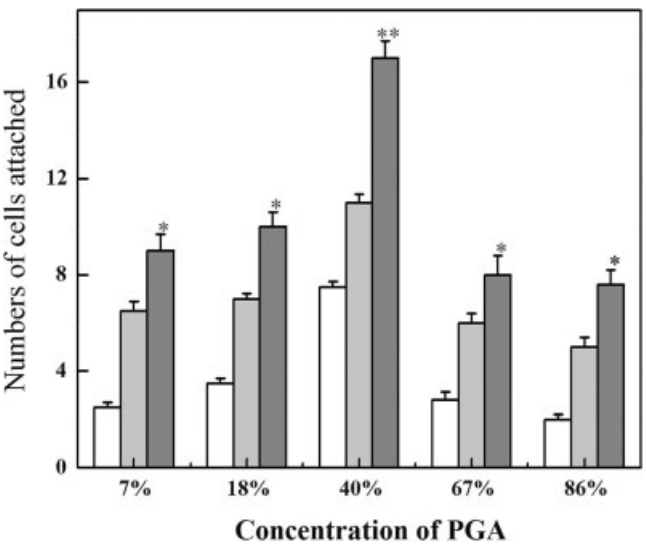

Figure 5. Relationship among the numbers of cells attached, concentrations of PGA, and fiber diameters. The numbers of cell attached were counted on the fibers with diameter of 10 μm (□); 3–5 μm (▭); 500 nm (■). There is a significant difference between the five groups of PGA concentrations and the number of cells attached. **, $p < 0.01$; The source of variance is in PGA/collagen mixing weight ration of 40% with different diameter scaffold 500 nm. *, $p < 0.05$ and **, $p < 0.01$. The numbers of cell attachment were counted on 25 independently aligned fibers. Error bars show the standard deviation.

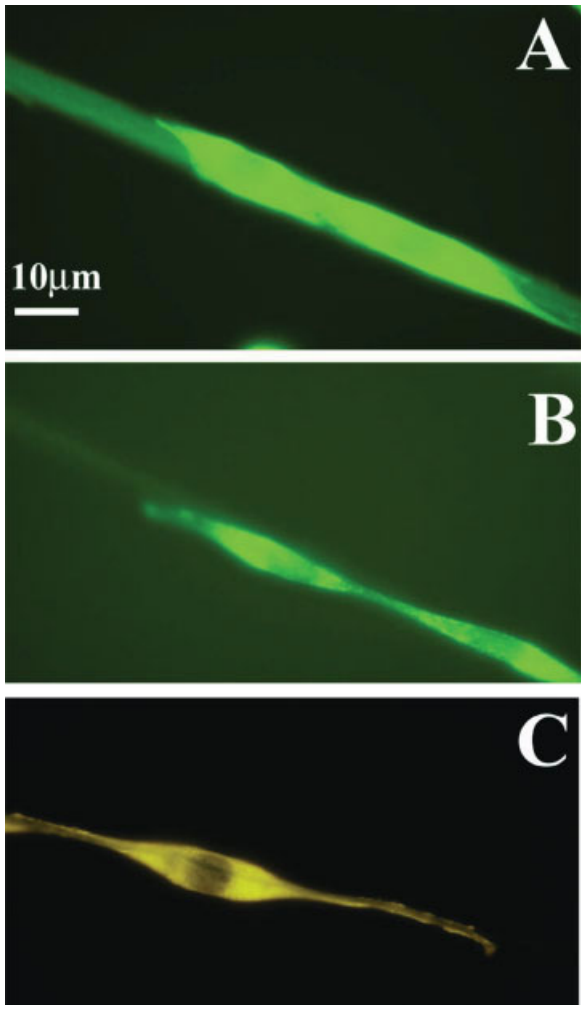

Figure 6. Fluorescent images of the morphology of cells on fibers. Images show cells spread on the PGA/collagen fibers of weight mixing ratio of 40% with the diameter of (A) 10 μm; (B) 3–5 μm; (C) 500 nm. [Color figure can be viewed in the online issue, which is available at www.interscience.wiley.com.]

the difficulties associated with cells interaction with multiple fibers in scaffolds, we developed an aligned electrospinning process in which the distance between the parallel fibers could be adjusted to eliminate "cell bridges" between multiple fibers. To minimize the interaction of cells and fibers with the substrate, we used a hydrophobic PVA substrate.[19] Since PVA is cell resistant under the conditions and time periods studied here, the interaction of cells was limited to the fibers. The distance between fibers was also controlled based on the collection time during the fabrication process. In the present study, the aligned fibers were collected on the drum of motor for 15 s to generate an interfiber distance greater than 200 μm. Therefore, the distance between the fibers enabled us to focus on the mechanisms of cell adhesion on individual fibers (Fig. 2).

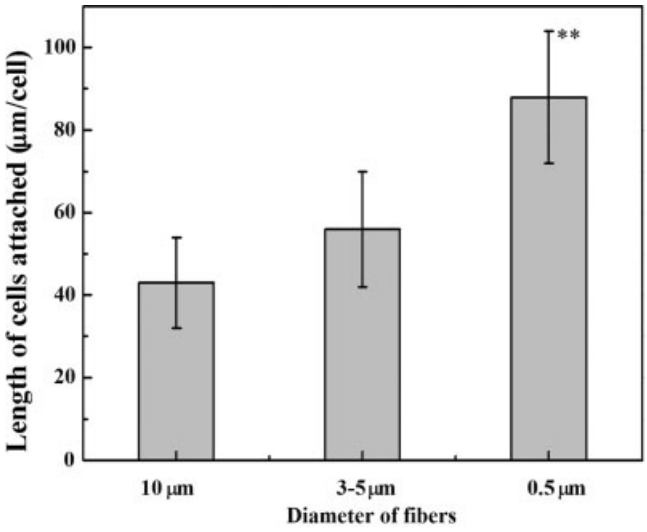

Figure 7. The relationship between length of attached cells and fiber diameters. The lengths of cells attached were measured on the fibers with diameter of 10 μm, 3–5 μm, and 500 nm. There is significant difference between fibers with diameter of 500 nm and other two groups. **, $p < 0.01$. The lengths of cells attached were measured on 25 independently aligned fibers. Error bars show the standard deviation.

The numbers of cells attached to fibers were found to be related to the number of cells that were seeded (Fig. 3). This is not surprising and demonstrates the

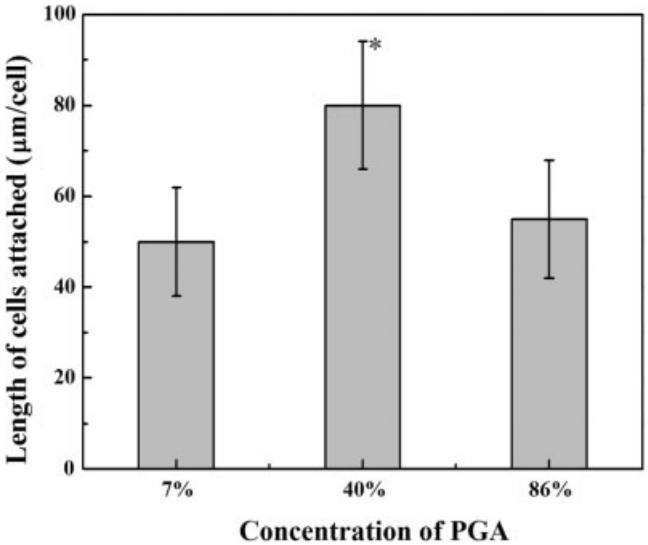

Figure 8. The relationship between lengths of cells attached and the concentrations of PGA. The cells were cultured in 10% FBS mediums for 8 h on different concentration of PGA fibers. The lengths of cells attached were measured on the fibers of PGA/collagen weight mixing ratio of 7, 40, and 86%. There is significant difference between fibers at the PGA/collagen weight mixing ratio of 40% with other two groups. *, $p < 0.05$. The lengths of cells attached were measured on 25 independently aligned fibers. Error bars show the standard deviation.

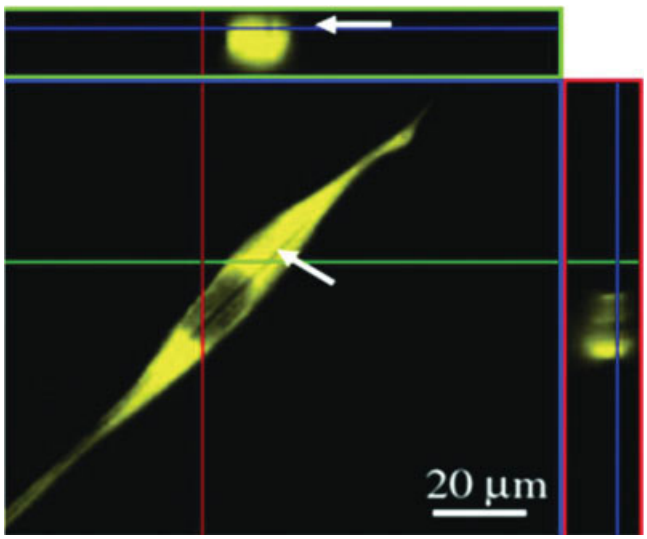

Figure 9. Confocal microscopy image shows cell interacting with a PGA/collagen nanofiber at PGA/collagen at weight mixing ratio of 40% in DMEM supplemented with 10% FBS for 8 h. In the middle of image, the cell shows spreading and aligning with the fiber with diameter of 500 nm (scale bar = 20 μm). On the top of the image, the dark area presents fiber area. The arrows show that the fiber is underneath the cell. [Color figure can be viewed in the online issue, which is available at www.interscience.wiley.com.]

importance of appropriate cell seeding density to minimize cell necrosis, while maximizing the number of cells in the tissue engineering constructs. In addition, it was observed that the number of NIH-3T3 fibroblasts was significantly increased as the diameter of the fibers decreased (Figs. 4 and 5). Thus, there was a significant difference ($p < 0.01$) between fibers with a diameter of 500 nm compared with those with diameter of 3–5 and 10 μm. Figures 6 and 7 clearly show that NIH-3T3 cells attached on the PGA/collagen fiber with smaller diameter are more spread than those seeded on bigger diameter. Cells attached to nanofibers appear to be more elongated and fibroblastic. Our observations are consistent with literature findings that cell growing on the smaller fibers are more spread and exhibit a cytoskeletal architecture that mimics cells growing on a glass surface.[5–7]

Morphological observations suggest a rather straightforward interpretation of the interplay of surface area and surface chemistry. The correlation between the cell behavior and different PGA/collagen composition in the scaffolds has not yet been studied well.[10] In the present study, the cell adhesion was evaluated on fibers with different PGA concentration in a quantitative way. Figures 7 and 8 show that those fibers with diameter of 500 nm and PGA/collagen weight mixing ratio of 40% provided the highest average length ($p < 0.01$) of cells attached to the fibers. The statistical analysis and experimental observations suggest that the highest number of attached cells (Fig. 5) and the longest average of cell length (Figs. 7 and 8) occur at PGA/collagen weight mixing ratio of 40%. There is a biphasic relationship between the cell adhesion and the PGA/collagen composition (Figs. 5 and 8). Therefore, the number and average length of cells attached decrease when the PGA/collagen weight mixing ratio decreases to 40%.

The drawback of collagen as a scaffold for cell proliferation and differentiation is its poor mechanical strength. To overcome the inherent nature of collagen as cells scaffold, the combination with other materials has been attempted.[10] In addition, the materials to be combined should be bioabsorbable, shapeable, and deformable. PGA fibers have the highest elastic module among the fibers and showed a much better retention of mechanical properties than collagen.[20–22] The ductility of PGA could improve the shapability of bioabsorbable composite device for skin-healing application.

It is well known that focal adhesion consists of clustered integrins and numerous membrane-associated and cytoplasmic molecules.[23] The surface chemistry plays an important role for cell adhesion. On the other hand, the surface topography affects cell attachment. A cell membrane containing diffusive mobile receptors wraps around a cylindrical fiber with compatible ligands. The receptor-ligand binding cause the membrane to locally wrap around the fiber at the cost of elevated elastic energy associated with increased locale curvature of the membrane and reduced change order associated with receptor immobilization. The theory of cell membrane is easy form curvature under the diameter of 320 nm.[24] Many research studies of cell have explained the mechanism by which cell respond to the aligned stripes and grooves.[25] Their experiments show cells keep stable at the stripes or grooves heights around 500 nm and show largest spreading area on the stripes width with 500 nm.[26] The matrix curvature directly affects the cell adhesion. Cellular membranes curvature can be dynamically modulated by changes in lipid composition.[27] Those evidences suggested that cellular membrane easily forms curvature in diameter of 500 nm. In present study, the diameter of cell membrane curvature is related with the diameters of fibers. The cell membrane curves in 500-nm tunnel and change conformation to tend to cylindrical spread following the fiber orientation. A particle-cell model for the mechanism of action based on changes in cell membrane curvature is shown in Figure 10. When the cell contacts with fiber, the receptors of cell membrane hold the ligands of fiber surface. A cell membrane holding receptors wraps around a cylindrical fiber with compatible ligands. The receptor–ligand binding causes the membrane to locally wrap around the fiber at

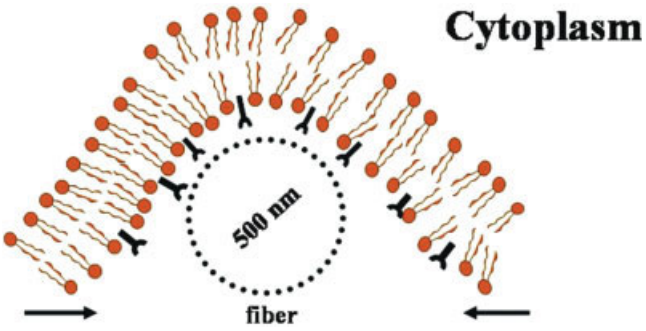

Figure 10. The mechanism of cell membrane curvature with cylindrical nanofiber. Diameter of fiber is 500 nm. A cell membrane holding receptors wraps around a cylindrical fiber with compatible ligands. The membrane locally wrap around the fiber to reduce free energy of interaction and increase local curvature of the membrane. [Color figure can be viewed in the online issue, which is available at www.interscience.wiley.com.]

the cost of elevated elastic energy associated with increased locale curvature of the membrane and reduced change order associated with receptor immobilization. Finally, the cell membrane starts changing the curvature and spreading. That is why this phenomenon does result in the cell membrane curves in 500-nm tunnel and change conformation to tend to cylindrical spread following the fiber orientation (Fig. 9). Consequently, the lengths of and number of cell attached are related with the diameters of fibers (Figs. 4, 5, and 7).

We presented here an analysis method of the relationship between the number and average length of NIH-3T3 attached to fibers with different diameters and composition on separate aligned fibers. The fiber diameters were controlled by electrospinning. This finding points out that a PGA/collagen weight mixing ratio of 40% and fiber diameter of 500 nm provided the best conditions for NIH-3T3 to adhere to the fibers. The separated aligned fiber structures could help to quantify the number of attached NIH-3T3 and their average length. This quantitative method can be employed to provide information to select the scaffold materials for skin-healing application.

CONCLUSIONS

A quantitative method was developed to evaluate the cell attachment affinity to aligned fibers composed of PGA and collagen. Our results clearly indicate that there is strong relationship among PGA/collagen composition, fiber diameter, and number of NIH-3T3 attached to fibers. This study indicates that the effect of nanofibers on the cells for better understanding of interactions of cells with nanomaterials. Such information would have important implications in selecting biomaterials for further applications.

We greatly appreciated technical assistance of Mrs. Takako Honda. We thank Dr. Adriele Prina-Mello (Centre for Research on Adaptive Nanostructures and Nanosciences, Trinity College, Dublin, Ireland) for reading the final manuscript.

References

1. Lamme EN, Leeuwen RTJV, Jonker A, Marle JV, Middelkoop E. Living skin substitutes: Survival and function of fibroblasts seeded in a dermal substitute in experimental wounds. J Invest Dermal 1998;111:989–995.
2. Zhong S, Teo WE, Zhu X, Beuerman RW, Ramakrishna S, Yue L, Yung L. An aligned nanofibrous collagen scaffold by electrospinning and its effects on in vitro fibroblast culture. JBiomed Mater Res A 2006;78:456–463.
3. Li WJ, Laurencin CT, Caterson EJ, Tuan RS, Ko FK. Electrospun nanofibrous structure: A novel scaffold for tissue engineering. J Biomed Mater Res A 2002;60:613–621.
4. Ma ZW, Kotaki M, Inai R, Ramakrishna S. Potential of nanofiber matrix as tissue-engineering scaffolds. Tissue Eng 2005; 11:101–109.
5. Takahashi Y, Tabata YJ. Effect of the fiber diameter and porosity of non-woven PET fabrics on the osteogenic differentiation of mesenchymal stem cells. J Biomater Sci Polym Ed 2004;15:41–57.
6. Li M, Guo Y, Wei Y, MacDiarmid AG, Lelkes PI. Electrospinning polyaniline-contained gelatin nanofibers for tissue engineering applications. Biomaterials 2006;27:2705–2715.
7. Yang F, Murugan R, Wang S, Ramakrishna S. Electrospinning of nano/micro scale poly(L-lactic acid) aligned fibers and their potential in neural tissue engineering. Biomaterials 2006; 26:2603–2610.
8. Yang F, Xu CY, Kotaki M, Wang S, Ramakrishna S. Characterization of neural stem cells on electrospun poly(L-lactic acid) nanofibrous scaffold. J Biomater Sci Polym Ed 2004;15: 1483–1497.
9. Boland ED, Telemeco TA, Simpson DG, Wnek GE, Bowlin GL. Utilizing acid pretreatment and electrospinning to improve biocompatibility of poly(glycolic acid) for tissue engineering. J Biomed Mater Res B 2004;71:144–152.
10. Rho KS, Jeong L, Lee G, Seo BM, Park YJ, Hong SD, Roh S, Cho JJ, Park WH, Min BM. Electrospinning of collagen nanofibers: Effects on the behavior of normal human keratinocytes and early-stage wound healing. Biomaterials 2006;27:1452–1461.
11. Li WJ, Danielson KG, Alexander PG, Tuan RS. Biological response of chondrocytes cultured in three-dimensional nanofibrous poly(ε-caprolactone) scaffolds. J Biomed Mater Res A 2003;67:1105–1114.
12. Katta P, Alessandro M, Ramsier RD, Chase GG. Continuous electrospinning of aligned polymer nanofibers onto a wire drum collector. Nano Lett 2004;4:2215–2218.
13. Wnek GE, Carr ME, Simpson DG, Bowlin GL. Electrospinning of nanofiber fibrinogen structures. Nano Lett 2003;3: 213–216.
14. Li D, Ouyang G, McCann JT, Xia Y. Collecting electrospun nanofibers with patterned electrodes. Nano Lett 2005;5:913–916.
15. Baker SC, Atkin N, Gunning PA, Granville N, Wilson K, Wilson D, Southgate J. Characterisation of electrospun polystyrene scaffolds for three-dimensional in vitro biological studies. Biomaterials 2006;27:3136–3146.

16. Linge C, Green MR, Brooks RF. A method for removal of fibroblasts from human tissue culture systems. Exp Cell Res 1989;185:519–528.
17. Tian F, Hosseinkhani H, Estrada GG, Kobayashi H. Quantitative method for the analysis of cell attachment using aligned scaffold structures. Proceedings of ICN+T 2006, submitted.
18. Tian F, Cui D, Schwarz H, Estrada GG, Kobayashi H. Cytotoxicity of single-wall carbon nanotubes on human fibroblasts. Toxicol In Vitro 2006;20:1202–1210.
19. Miyashita H, Shimmura S, Kobayashi H, Taguchi T, Asano-Kato N, Uchino Y, Kato M, Shimazaki J, Tanaka J, Tsubota K. Collagen-immobilized poly(vinyl alcohol) as an artificial cornea scaffold that supports a stratified corneal epithelium. J Biomed Mater Res B 2006;76:56–63.
20. Murugan R, Ramakrishna S. Nano-featured scaffolds for tissue engineering: A review of spinning methodologies. Tissue Eng 2006;12:435–447.
21. Slivka MA, Chu CC. Fiber-matrix interface studies on bioabsorbable composite materials for internal fixation of bone fractures. I. Raw material evaluation and measurement of fiber-matrix interfacial adhesion. J Biomed Mater Res 1997;37: 353–362.
22. Hutmacher DW, Schantz T, Zein I, Ng KW, Teoh SH, Tan KC. Mechanical properties and cell cultural response of polycaprolactone scaffolds designed and fabricated via fused deposition modeling. J Biomed Mater Res 2001;55:203–216.
23. Calvacanti-Adam EA, Micoulet A, Blümmel J, Auernheimer J, Kessler H, Spatz JP. Lateral spacing of integrin ligands influences cell spreading and focal adhesion assembly. Eur J Cell Biol 2006;85:219–224.
24. Gao HJ, Shi D, Freund LB. Mechanics of receptor-mediated endocytosis. Proc Natl Acad Sci USA 2005;102:9469–9474.
25. Jungbauer S, Kemkemer R, Gruler H, Kaufmann D, Spatz JP. Cell shape normalization, dendrite orientation, and melanin production of normal and genetically altered (Haploinsufficient NF1)-melanocytes by microstructured substrate interactions. Chem Phys Chem 2004;5:85–92.
26. Uttayarat P, Toworfe GK, Dietrich F, Lelkes PI, Composto RJ. Topographic guidance of endothelial cells on silicone surfaces with micro- to nanogrooves: Orientation of actin filaments and focal adhesions. J Biomed Mater Res A 2005;75:668–680.
27. McMahon HT, Gallop JL. Membrane curvature and mechanisms of dynamic cell membrane remodeling. Nature 2005; 4381:590–596.